PHYSICAL REVIEW C VOLUME 46, NUMBER 1 JULY 1992

Spin-triplet strength in the $^3H(\vec{p},\gamma)^4He$ reaction at $E_p = 2$ MeV

W. K. Pitts
University of Wisconsin–Madison, Madison, Wisconsin 53706
(Received 29 August 1991)

The cross section $\sigma(\theta)$ and analyzing power $A_y(\theta)$ of the $^3H(\vec{p},\gamma)^4He$ reaction have been measured at an incident proton energy $E_p = 2.00$ MeV. The angular distribution of the spin-dependent cross section $\sigma(\theta)A_y(\theta)$ shows that both odd parity ($E1$) and even parity ($E2, M1$) transitions contribute to this reaction. Detailed matrix element fits result in a spin-triplet total cross section which is $0.72(+0.29, -0.18)\%$ of the total $^3H(\vec{p},\gamma)^4He$ reaction cross section. A nucleon-only calculation does not reproduce the data, and predicts a spin-triplet total cross section which is only 0.01% of the total cross section. The inclusion of meson exchange currents into this calculation increases the spin-triplet cross section to 0.5% of the total cross section, in agreement with the present results. A comparison of the calculated and fitted matrix elements is presented.

PACS number(s): 25.10.+s, 25.40.Lw

Much of the current interest in radiative capture reactions in the few-body systems centers around the effects of meson exchange currents (MEC) in nuclei. While Siegert's theorem can be used to write the spin-independent electric operator in a form which includes the pion exchange current, the theorem cannot be used for either the magnetic operator or the spin-dependent component of the electric operator [1]. In the case of the $^3H(\vec{p},\gamma)^4He$ reaction, the matrix elements most sensitive to MEC effects all have an entrance channel spin $S=1$ (spin triplet). These spin-triplet matrix elements are all much smaller than the dominant transition, the non-spin-flip electric dipole transition ($^1P_1$ $E1$, in spectroscopic notation). A nucleon-only calculation showed that the sum of the spin-triplet partial cross sections was only 0.01% of the total cross section at an incident proton energy $E_p = 2$ MeV [2]. This calculation did not include MEC effects, and the only D-state component was that included in the $d+d$ cluster wave function. The later inclusion of D-state components in the ^2H, ^3He, and ^3H clusters resulted in larger spin-triplet matrix elements, especially for the very small $^3S_1$ $M1$ and $^3D_2$ $E2$ transitions [3]. The total cross section in the spin-triplet channel did not significantly increase, however, since the largest spin-triplet transition, the $^3P_1$ $E1$, had only a small increase from the D-state components. The determination of the spin-triplet total cross section typically requires the measurements of an interference effect with the dominant spin-singlet channel. An observable of this type is the spin-dependent cross section $\sigma(\theta)A_y(\theta)$, which is dominated by the interference between spin-triplet and spin-singlet transitions. Disagreement between a precise measurements of $\sigma(\theta)A_y(\theta)$ and calculations such as those described above could then be interpreted as evidence of MEC or D-state contributions to this reaction.

The determination of the $^3S_1$ $M1$ matrix element in the $^3H(\vec{p},\gamma)^4He$ reaction would be especially interesting. The one-body spin-flip component of the $M1$ operator is restricted to act only between the D states of both the ^3He and ^4He nuclei, first shown for the isospin-conjugate $^3He(n,\gamma)^4He$ reaction [4]. The resulting matrix element is then small and dominated by MEC effects. Recent calculations show that the mesonic degrees of freedom could be responsible for as much as 90% of the $^3He(n,\gamma)^4He$ total cross section at thermal neutron energies [5,6]. An order of magnitude estimate of the expected $M1$ total cross section for the $^3H(\vec{p},\gamma)^4He$ reaction at $E_p = 2.00$ MeV can be derived in the following way. An energy independent matrix element for the $^3He(n,\gamma)^4He$ $M1$ transition would result in a $1/v$ energy dependence of the $^3S_1$ $M1$ total cross section. Scaling an average of thermal neutron capture cross sections to an incident energy $E_n = 2$ MeV gives a total $M1$ cross section of about 0.004 μb [6]. The total cross sections for the $^3He(n,\gamma)^4He$ and $^3H(\vec{p},\gamma)^4He$ reactions are related by isospin invariance, and the total cross section for the $^3H(\vec{p},\gamma)^4He$ reaction at $E_p = 2$ MeV is about 40 μb [7]. The resulting $M1$ cross section is estimated to be of the magnitude of 0.01% of the total cross section for the $^3He(n,\gamma)^4He$ reaction at $E_n = 2$ MeV.

A previous measurement of this reaction at $E_p = 2$ MeV has been interpreted as evidence of an $M1$ total cross section much larger than the 0.01% estimate derived above [8]. They fitted both $\sigma(\theta)$ and $\sigma(\theta)A_y(\theta)$ data using the $^1P_1$ $E1$, $^3P_1$ $E1$, $^1D_2$ $E2$, and $^3S_1$ $M1$ transition matrix elements. The effect of the spin-triplet $^3D_2$ $E2$ transition was ignored, however, since nucleon-only calculations without any D-state component predicted that this matrix element would be negligible. The effect of the $^3D_2$ $E2$ transition upon the analyzing power can be similar to that of the $^3S_1$ $M1$ transition, however, and in particular upon that component of $A_y(\theta)$ which is symmetric about 90°. The $M1$ total cross section resulting from this fit was on the order of 1% of the total cross section at proton energies of $E_p = 0.86$, 2, and 5 MeV. The data at 0.86 MeV were generated by combining a new measurement of $\sigma(\theta)$ with previously measured analyzing power data [9]. Taken at face value, this result would imply a very large MEC contribution for this transition.

 ©1992 The American Physical Society

A measurement of significantly better precision would yield new and interesting information concerning the spin dependence of the reaction and possible MEC effects. The measurement described here was carried out at an incident proton energy $E_p = 2$ MeV ($E_\gamma = 21.25$ MeV), reducing the effect of the $^1P_1$-$^3P_1$ $E1$-$E1$ interference which dominates $A_y(\theta)$ at higher energies [10]. There are also no nearby states which have an $E1$, $E2$, or $M1$ photon decay to the ground state. The ^{4}He state at an excitation energy of 21.84 MeV has quantum numbers 2^- ($T=0$), and only isoscalar $M2$ radition would be expected from this state. Direct $M2$ radiation should be suppressed by the angular momentum barrier, and is ignored in the analysis below. Further details of the present measurement and additional $^3\mathrm{H}(\vec{p},\gamma)^4\mathrm{He}$ data at higher energies will be provided in another paper [11].

This experiment was performed at the University of Wisconsin using a sodium iodide (NaI) spectrometer and a tritium gas target of thickness 1.1 mg/cm^2. The polarized beam was produced in an atomic beam source with ionization in a cesium beam [12]. The beam polarization was typically 0.87 with a daily drift of less than ± 0.01. The polarimeter was based upon the $^4\mathrm{He}(\vec{p},p)^4\mathrm{He}$ reaction, and was calibrated to an accuracy of 2%. The beam position was stabilized using feedback from slits upstream of the target. The last beam definition element before the target was a tantalum collimator with an inner diameter of 2.0 mm located 16.9 cm upstream of the target entrance foil. The collimator was aligned to within 0.1 mm of the line defined by the beamline alignment target and the spectrometer center of rotation. The main body of the tritium target was a stainless steel tube of outer diameter 7.9 mm and wall thickness 0.8 mm. The tube was lined with a 125 μm tantalum foil and has an internal gold beam stop 0.51 mm thick. The entrance window was a 2.5 μm molybdenum foil. Two tritium cells were used for these measurements, one of effective length 52.0 mm and the other 51.7 mm. The respective centers of the tritium targets were upstream of the spectrometer center of rotation by 0.3 ± 0.2 mm and 0.2 ± 0.2 mm. This offset includes the outward bowing of the entrance foil, and the quoted uncertainty is dominated by the estimated uncertainty in the bowing. The data were taken at eight different angles, ranging from $\theta = 0°-155°$. The spectrometer was rotated to either side of the beamline for measurements, and data were accumulated on both sides of the incident beam except for $\theta = 135°$ and $\theta = 155°$. These angle settings were blocked on one side by interference between the spectrometer shield and the tritium furnace. A 16.9 g/cm^2 paraffin block in front of the spectrometer collimator outscattered most neutrons from the target. Dead time was measured with a pulser triggered at a rate proportional to the beam current. The pulser was adjusted to have the same shape as true signals, thus giving an accurate monitor of pileup rejection.

Typical spectra at dector angles of 0° and 90° are shown in Fig. 1. The spectra were fitted by a combination of three skewed Gaussians (one each for the photopeak and first and second escape peaks), an exponential pileup tail above the peak, an exponential escape tail below the peak, and a background which consisted of both a flat and exponential component [13]. The analyzing power of the exponential background was a parameter of the fit. The fit is constructed for the purpose of giving a determination of the background. The yield is taken from the number of counts contained in the summation region (chosen to include 90% to 103% of the photopeak channel) minus the background determined from the fit. The typical background was no more than 2% of the peak sum except at 0°, where the background was about 7%. Empty target spectra were not measured since the $^3\mathrm{H}(p,n)^3\mathrm{He}$ reaction was the dominant source of the background.

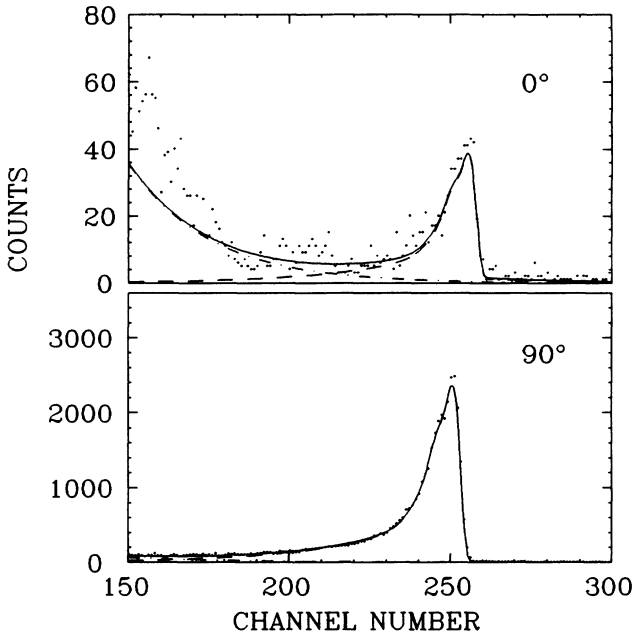

FIG. 1. Typical spectra at detector angles of 0° and 90°. The dashed curve is the fit to the peak, the dot-dashed curve is the background, and the solid curve is the sum of the two.

Since the primary use of these measurements is to determine the transition matrix element by fitting $\sigma(\theta)$ and $\sigma(\theta)A_y(\theta)$, most systematic corrections are important only as they affect the shape of the angular distribution about 90°. The largest systematic correction resulted from the angular dependence of the photon absorption in the inhomogeneous target wall. The absorption was calculated by averaging the photon absorption over all possible paths from the target to the spectrometer. A $\sin^2\theta$ weight was added to correct for the variation of the angular distribution of the reaction over the face of the spectrometer. The calculated attenuation was within 10% of that expected from a uniform tube, except at detector angles of $\theta = 0°$ and $\theta = 155°$. The correction at these angles was increased by absorption in the beam stop and welded joint, respectively. The correction was applied to the data as a multiplicative factor, which was set equal to the ratio of the surviving fraction at angle θ with respect to that at 90°. The uncertainty is conservatively estimated to be $\pm 10\%$ of the difference between the correction and unity. The maximum loss at any angle was estimated to be 8% at $\theta = 155°$. The resulting systematic uncertainty

in $\sigma(155°)$ was $\pm 0.8\%$, which was about twice the statistical uncertainty of the data point. No correction was made for the change of spectrometer efficiency with reaction angle and energy. The Q value of this reaction is 19.81 MeV, and the resulting range of photon energies at $E_p = 2$ MeV is 20.9 to 21.6 MeV. An estimate of the maximum efficiency shift between forward and backward angles shows that the effect is much smaller than the statistical uncertainty of the data at the extreme angles.

A systematic correction was needed to account for the decrease of the tritium content of the target with time. The relative change of the tritium content of the cell was extracted from the 90° yield as a function of time, with the uncertainty determined by the $\pm 1\sigma$ errors in the fit. Over the course of the three data runs the decrease of the target thickness was 9.5%, 4.1%, and 3.9%. The correction did not significantly alter either the shape of the angular distribution or the extracted fitting coefficients since the detector position was changed often on the time scale of the target density decrease.

The systematic correction that most influences the extracted spin-triplet matrix elements results from an effective shift of the centroid of the gas target along the beam axis. One correction accounts for the misalignment of the target centroid with respect to the spectrometer center of rotation, which also generates a shift of at most 0.03° in the scattering angle. A second correction is required due to the change of the yield with energy loss in the tritium gas, where the excitation function was taken from the work of Perry and Bame [14]. Both of these effects were analytically calculated for a point detector. Each of these corrections had approximately equal effects upon $\sigma(\theta)$. The combined effect of both corrections was small, with a maximum fractional correction of -4.3×10^{-3} at $\theta = 155°$. The uncertainty of the correction to $\sigma(\theta)$ was estimated to be less than 6×10^{-4} of the value of $\sigma(\theta)$, and is determined by repeating the calculation for the maximum position uncertainty. An additional correction would be required if there was a significant adsorption of tritium upon the entrance foil or beam stop. While this effect was not directly measured, an order of magnitude estimate can be derived. The tritium target was measured to have a maximum loss of 10% over one week. An upper limit is found by assuming that the lost tritrium is adsorbed uniformly onto all the walls of the cell except at the entrance foil. The resulting shift of the yield between $\sigma(0°)$ and $\sigma(180°)$, measured at the end of the week, is then only 5×10^{-4}. Since most of the data were acquired with a target loss of only 4% during a one week data run, the above estimate represents a very conservative upper bound.

The systematic erorrs on the fitting coefficients were determined by forming data sets with data points shifted according to the maximum and minimum variation of the corrections. The effects of photon attenuation, longitudinal misalignment, and yield variation can contribute coherently, and data sets with combinations of these effects were propagated through the analysis. The sets of data that were shifted by the uncertainty in the time-dependent tritium variation were also propagated through the analysis. Each of these shifted data sets was then fit in the same way as the nominal data set.

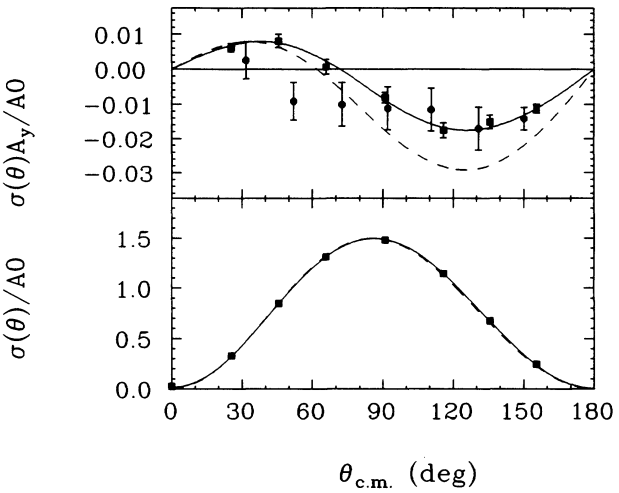

FIG. 2. The results of this experiment shown as squares. The size of the square is larger than the estimated error for $\sigma(\theta)$. The circles are the results of Wagenaar *et al.* [8]. The solid curve is fit *B*, Table II. The dashed curve is column "Theory II" of Table II [3].

The results of this measurement are shown in Fig. 2 as squares. The error estimates include only the statistical uncertainty. The round dots are the $\sigma(\theta)A_y(\theta)$ results of Wagenaar *et al.* at 2.00 MeV. The curves are fits using the Legendre function expansions

$$\sigma(\theta) = A_0 \left[1 + \sum Q_i a_i P_i(\cos\theta)\right], \quad (1)$$

$$\sigma(\theta)A_y(\theta) = A_0 \left[\sum Q_i b_i P_i^1(\cos\theta)\right], \quad (2)$$

where $\sigma_{\text{tot}} = 4\pi A_0$ and the index i ranges from 1 to 4. This fitting form has the advantage that the a_i and b_i coefficients can ultimately be expressed as a sum of products of allowed reaction amplitudes [15]. The Q_i's are the finite geometry corrections due to the finite detector size, extended target, and multiple scattering in the entrance foil [16,17]. The prescription of Dixon *et al.* was used to generate the multiple scattering distribution [18]. The fitting coefficients were determined by simultaneously fitting both the $\sigma(\theta)$ and $\sigma(\theta)A_y(\theta)$ data. The a_i and b_i coefficients are listed in Table I. The χ^2 of the best fit is 5.10. The reduced χ^2 is 0.85. The first quoted uncertainty is the statistical uncertainty, including the effects of correlations between the coefficients. This uncertainty is defined such that shifting the coefficient by the uncertainty, and then optimizing the fit to the remaining coefficients, results is an increase of 1 in the χ^2. The second quoted uncertainty is the systematic uncertainty in the coefficient. It is defined as the maximum positive and negative changes in the coefficient which result from fitting data sets which are shifted by the uncertainties in the systematic corrections described above. The results of Ref. [8] are also listed in Table I.

There are qualitative features of the reaction evident in these a_i and b_i coefficients. The dominant $^1P_1$ $E1$ transition is seen in $a_2 \approx -1$. The spin-triplet and spin-singlet

TABLE I. Expansion coefficients from a simultaneous fit to $\sigma(\theta)$ and $\sigma(\theta)A_y(\theta)$ at $E_p=2$ MeV. The quoted errors are the statistical and systematic uncertainties, respectively. The column labeled "TUNL Data" are the results of Wagenaar *et al.* [8].

Coefficient	Present Data	TUNL Data
a_1	$0.0811^{+0.0009\ +0.0005}_{-0.0009\ -0.0004}$	0.069±0.005
a_2	$-0.9826^{+0.0009\ +0.0020}_{-0.0009\ -0.0020}$	−0.981±0.005
a_3	$-0.0771^{+0.0014\ +0.0011}_{-0.0014\ -0.0011}$	−0.060±0.009
a_4	$-0.0063^{+0.0014\ +0.0010}_{-0.0014\ -0.0011}$	−0.011±0.010
b_1	$-0.0076^{+0.0009\ +0.0000}_{-0.0009\ -0.0000}$	−0.013±0.003
b_2	$0.0080^{+0.0007\ +0.0000}_{-0.0007\ -0.0000}$	0.003±0.002
b_3	$0.0004^{+0.0004\ +0.0000}_{-0.0004\ -0.0000}$	0.000±0.001
b_4	$-0.0001^{+0.0004\ +0.0000}_{-0.0004\ -0.0000}$	0.002±0.001

transitions do not interfere in $\sigma(\theta)$, and $a_1 \approx -a_3$ shows the influence of the $^1P_1$-$^1D_2$ $E1$-$E2$ interference. The presence of $E2$ radiation is confirmed in the a_4 coefficient. The effect of the spin-triplet strength is seen most clearly in the nonzero b_1 and b_2 coefficients. Assuming that the dominant terms are those which interfere with the large $^1P_1$ $E1$ amplitude, the b_2 coefficient is likely due to a $^1P_1$-$^3P_1$ $E1$-$E1$ interference and the b_1 coefficient is likely due to the $^3S_1$ $M1$ or the $^3D_2$ $E2$ transitions. It is clear from Table I that at least four transitions contribute.

The $\sigma(\theta)$ and $\sigma(\theta)A_y(\theta)$ data have been directly fit using transition amplitudes [15]. The amplitudes used in the fit have a normalization such that

$$\sigma_{\text{tot}}=0.75[|^1P_1|^2(E1)+|^3P_1|^2(E1)+|^3S_1|^2(M1)+|^3D_1|^2(M1)]+1.25[|^1D_2|^2(E2)+|^3D_2|^2(E2)]\ . \quad (3)$$

There are nine coefficients resulting from a fit of Legendre functions to the $\sigma(\theta)$ and $\sigma(\theta)A_y(\theta)$ data if only multipoles of rank 2 or less contribute. The $^1P_1$ $E1$ phase is set to zero, and five matrix elements and four relative phases can be determined.

The first set of fitting matrix elements was the same as that chosen by Wagenaar *et al.* [8]. The results of this fit using only the $^1P_1$ $E1$, $^3P_1$ $E1$, $^1D_2$ $E2$, and $^3S_1$ $M1$ transitions (i.e., no $^3D_2$ $E2$ contribution) are shown in the column labeled "Fit A" of Table II. Each of the transition matrix elements has been normalized to the large $^1P_1$ $E1$ matrix element. The χ^2 of this fit is 5.21, in excellent agreement with the empirical fit of Table I. The results of the fit are also in excellent agreement with those published by Wagenaar *et al.* [8]. In particular, the resulting $M1$ total cross section (including both statistical and systematic uncertainties) is 1.09±0.22 % of the total cross section, while Wagenaar *et al.* find a value of 1.2±0.8 %. While the low χ^2 indicates a good fit to the data, there are some indications that this set of matrix elements may not

TABLE II. Matrix elements and phases from fits A and B (described in the text). The quoted errors are the statistical and systematic uncertainties, respectively. The $^1P_1$ phase, $\phi(^1P_1)$, was defined to be zero and the amplitudes have been normalized to the $^1P_1$ $E1$ amplitude. The angles are in radians. The calculated matrix elements in the column "Theory I" are the result of a nucleon only resonating group calculation [2], while those in the column "Theory II" include MEC effects [3].

Coefficient	Fit A	Fit B	Theory I	Theory II
$^1P_1$ $E1$	$1.000^{+0.000\ +0.000}_{-0.000\ -0.000}$	$1.000^{+0.000\ +0.000}_{-0.000\ -0.000}$	1.000	1.000
$^3P_1$ $E1$	$0.016^{+0.005\ +0.004}_{-0.004\ -0.004}$	$0.085^{+0.005\ +0.004}_{-0.006\ -0.005}$	0.008	0.067
$^1D_2$ $E2$	$0.047^{+0.005\ +0.005}_{-0.005\ -0.005}$	$0.047^{+0.005\ +0.004}_{-0.005\ -0.004}$	0.024	0.028
$^3D_2$ $E2$	(not fit)	$0.006^{+0.005\ +0.000}_{-0.003\ -0.001}$	3×10^{-4}	9×10^{-5}
$^3S_1$ $M1$	$0.105^{+0.006\ +0.005}_{-0.006\ -0.005}$	$0.009^{+0.018\ +0.006}_{-0.009\ -0.003}$	0.002	0.014
$^3D_1$ $M1$	(not fit)	(not fit)	4×10^{-4}	6×10^{-4}
$\phi(^3P_1)$ $E1$	$3.06^{+0.08\ +0.11}_{-0.12\ -0.08}$	$0.14^{+0.03\ +0.02}_{-0.02\ -0.01}$	2.17	2.88
$\phi(^1D_2)$ $E2$	$1.07^{+0.05\ +0.04}_{-0.08\ -0.06}$	$1.07^{+0.06\ +0.04}_{-0.08\ -0.05}$	0.09	0.09
$\phi(^3D_2)$ $E2$	(not fit)	$0.61^{+1.81\ +0.17}_{-0.31\ -0.05}$	0.14	−3.03
$\phi(^3S_1)$ $M1$	$0.046^{+0.007\ +0.002}_{-0.007\ -0.002}$	$-2.93^{+2.68\ +0.33}_{-0.14\ -0.16}$	0.86	0.83
$\phi(^3D_1)$ $M1$	(not fit)	(not fit)	−2.99	0.02

be a complete description of the physics of this reaction. Note first that this $M1$ cross section is two orders of magnitude larger than that expected from the velocity extrapolation of the $^3He(n,\gamma)^4He$ thermal neutron cross section. The $^3P_1$ $E1$ matrix element is very small and almost entirely real, in dramatic contrast to the situation at higher energies [8]. The largest contribution to the b_2 coefficient in this fit is not that from $^3P_1$-$^1P_1$ $E1$-$E1$ interference, but instead is that from the $^3S_1$-$^1D_2$ $M1$-$E2$ interference. The $^3S_1$ $M1$ transition is responsible for nearly all the spin-triplet features in this fit.

The $^3D_2$ $E2$ transition was then added to the above combination of matrix elements yielding a χ^2 of 5.04. The results of this fit are shown in Fig. 2 and listed in Table II as column *B*. Note that the very small $^3D_2$ $E2$ transition has a large effect upon the fit, resulting in a shift of the fitted spin-triplet strength from the $^3S_1$ $M1$ to the $^3P_1$ $E1$ transition. The resulting $M1$ total cross section is now on the order of 0.01% of the total cross section, in agreement with the estimate derived from the extrapolation of the thermal neutron capture data. The $^3P_1$ $E1$ matrix element is the largest spin-triplet matrix element, with a nonzero imaginary component. While the statistical quality of the data was not sufficient to determine the $^3S_1$ $M1$ and $^3D_2$ $E2$ matrix elements to high precision, both are small compared to the $^3P_1$ $E1$ matrix element which dominates the total spin-triplet cross section. The total spin-triplet cross section is 0.72 $(+0.29, -0.18)$% of the $^3H(\vec{p},\gamma)^4He$ total cross section. The $^3P_1$ $E1$ transition accounts for 99% of this measured strength. The $E2$ total cross section is 0.38 (± 0.14)% of the total cross section. Both the spin-triplet and $E2$ total cross sections are well determined. The error estimates of these cross sections have been generated by adding the statistical and systematic uncertainties in the matrix elements.

These results illustrate the need for a comprehensive theoretical analysis of this process. Existing nucleon-only calculation do not succeed in reproducing these new data. Column "Theory I" in Table II shows the matrix elements for a recent nucleon-only calculation [2]. The calculated spin-triplet matrix elements are all much smaller than the corresponding experimental results. The addition of explicit MEC effects increases the spin-triplet matrix elements ("Theory II" in Table II) by nearly an order of magnitude [3]. This calculation is shown as the dashed curve in Fig. 2, and it reproduces many of the qualitative features of the data. The most serious discrepancy is that the calculated $^3P_1$ $E1$ phase differs in sign from the measurement, indicating a possible problem with the calculation. The calculated $^3D_2$ $E2$ matrix element is significantly smaller than the measurement; however, a similar calculation with *D*-state components in all clusters, but with neglect of MEC effects, increases the $^3D_2$ $E2$ matrix element by an order of magnitude [3]. The features of these limited calculations suggest that a full treatment of this reaction, i.e., simultaneous treatment of both MEC and *D*-state effects, may result in a quantitative agreement with these new data.

It is clear from these data that the spin-triplet transitions are much larger than expected on the basis of nucleon-only calculations. While it is encouraging that new calculations are in qualitative agreement with the magnitude of the larger matrix elements, the measured and calculated phases significantly disagree and illustrate the need for additional theoretical effort.

I would like to thank Mr. Matt Devlin and the University of Wisconsin students who assisted in the measurement. Mr. Terry Morkved's assistance with the analysis was very much appreciated. I would also like to acknowledge the helpful comments of Prof. Lynn Knutson. Prof. H. M. Hofmann was kind enough to furnish the numerical values of the matrix elements. The National Science Foundation supported this work through Grants PHY-8717764 and PHY-0199983.

[1] Judah M. Eisenberg and Walter Greiner, in *Nuclear Theory, Volume 2: Excitation Mechanisms of the Nucleus* (North-Holland, Amsterdam, 1970), pp. 106–111.
[2] B. Wachter, T. Mertelmeier, and H. M. Hofmann, Phys. Rev. C **38**, 1139 (1988).
[3] H. M. Hofman, private communication.
[4] C. Werntz and B. G. Brennan, Phys. Rev. **157**, 759 (1967).
[5] J. Carlson *et al.*, Phys. Rev. C **42**, 830 (1990).
[6] R. Wervelman *et al.*, Nucl. Phys. **A526**, 265 (1991).
[7] G. Feldman *et al.*, Phys. Rev. C **42**, 1167 (1990).
[8] D. J. Wagenaar *et al.*, Phys. Rev. C **39**, 352 (1989).
[9] D. Krämer, W. Arnold, H. Berg, and G. Clausnitzer, in *Proceedings of the Fifth International Symposium on Polarization Phenomena in Nuclear Physics, Sante Fe, 1980,* AIP Conf. Proc. No. 69, edited by G. G. Ohlson, R. E. Brown, N. Jarmie, W. W. McNaughton, and G. M. Hale (AIP, New York, 1981), p. 1258.
[10] D. J. Wagenaar *et al.*, Phys. Rev. C **32**, 2155 (1985).
[11] W. K. Pitts and M. Devlin, in preparation.
[12] W. Haeberli *et al.*, Nucl. Instrum. Methods **196**, 319 (1982).
[13] T. R. Wang *et al.*, Phys. Rev. C **37**, 2301 (1988).
[14] J. E. Perry, Jr. and S. J. Bame, Jr., Phys. Rev. **99**, 1368 (1955).
[15] R. G. Seyler and H. R. Weller, Phys. Rev. C **20**, 453 (1979).
[16] M. E. Rose, Phys. Rev. **91**, 610 (1953).
[17] E. A. Heighway and J. D. MacArthur, Nucl. Instrum. Methods **79**, 224 (1970).
[18] D. R. Dixon *et al.*, IEEE Trans. Nucl. Sci. **NS-28**, 1295 (1981).